J Musculoskelet Neuronal Interact 2009; 9(2):109-120

Original Article

Hylonome

Effect of monosodium olpadronate on osteoclasts and megakaryocytes: An *in vivo* study

N.D. Escudero, M. Lacave, A.M. Ubios, P.M. Mandalunis

Cátedra de Histología y Embriología, Facultad de Odontología de la Universidad de Buenos Aires. Marcelo T de Alvear 2142 1º piso sector A. (C1122 AAH) Ciudad Autónoma de Buenos Aires, Buenos Aires, Argentina

Abstract

Bisphosphonates (BPs) are widely used to treat several bone pathologies. Their action on bone cells depends on cell lineage, promoting or preventing apoptosis in osteoclastic and osteoblastic lineage respectively. Bone cells and bone marrow (BM) are closely related. Bone marrow megakaryocytes regulate bone turn-over. The objective of this *in vivo* experimental work was to evaluate the effect of olpadronate (OPD) on osteoclasts (Ocs) and megakaryocytes (Mks) using histomorphometric, histochemical, and immunohistochemical methods. Healthy female Wistar rats were used: experimental and Sham animals received OPD or vehicle during five weeks. After sacrifice, kidneys, liver, spleen, femurs and tibiae were dissected and fixed for histological processing. H&E, histochemical detection of TRAP and immunohistochemical detection of TUNEL and RANKL were performed. Results showed increased bone volume and number of Ocs, larger Ocs with more nuclei, increase in Oc apoptosis, and loss of polarity in OPD-treated animals. Statistically significant association was found between apoptotic morphology and RANKL expression in Ocs. BM and spleen showed a significant increase in Mk number. The number of RANKL+Ocs and MKs per unit area increased. The increase in Oc apoptosis did not counteract the increase in Oc recruitment thus resulting in an increase in Oc number. Ocs recruitment could be associated with RANKL expression in Mks and apoptotic Ocs. The effect of OPD and other BPs on Mks should be investigated further to elucidate the mechanism by which BPs act on the bone-bone marrow functional unit, and understand the therapeutic implications of BPs.

Keywords: Bisphosphonates, Osteoclast, Megakaryocyte, RANKL, Bone Remodelling

Introduction

Over the last decades, bisphosphonates (BPs) have become the choice drug for treatment of osteoporosis and other bone diseases. They inhibit bone resorption through their effect on osteoclasts (Ocs), the cells in charge of bone resorption. Non-nitrogen-containing BPs (non-N-BPs) exert their effect by metabolizing intracellularly to non-hydrolyzable toxic analogues of ATP and leading to Oc death through apoptosis[1]. Nitrogen-containing BPs (N-BPs) that cannot be metabolized, interfere with the action of farnesil phosphate synthetase, an enzyme of the mevalonate pathway[2-4]. Loss of the cytoskeletal integrity of the cell and of the ruffled border is observed[5-7], and the Ocs become inactive reaching cell death through apoptosis[8,9]. Both N-BPs and non-N-BPs would reduce the number of Ocs, inhibiting recruitment or inducing apoptosis through different mechanisms thus resulting in a decrease in bone resorption and bone turnover. Experimental and clinical studies have shown a decrease in serum bone formation (alkaline bone phosphatase and osteocalcin, among others) and resorption markers (CTX and TRAP b5)[10,11] demonstrating this effect.

Bone and bone marrow (BM) constitute a functional unit[12]. An example of this relation is that osteoblasts (Obs) originate from non-hemopoietic stem cells in the bone marrow and Ocs originate from hemopoietic cells that are also in the BM. Thus, a number of relations between the osteoblastic niche in the bone and the vascular niche in the BM, where stem cells migrate in two directions, have been described[13]. Non-osteogenic cells in the BM, such as lymphocytes and megakaryocytes (Mks) are capable of releasing bone turnover regulating cytokines. Mks express several of these factors, such as osteoprotegerin (OPG)[14,15] and the

The authors have no conflict of interest.

Corresponding author: Dr. Mandalunis, Patricia, M.T. de Alvear 2142, Buenos Aires 1122, Argentina
E-mail: patricia@histo.odon.uba.ar

Accepted 3 February 2009

receptor activator of nuclear factor κβ ligand (RANKL)[15,16]. The binding of RANKL to its receptor RANK, (expressed by Oc precursors and mature Ocs) stimulates recruitment of new Ocs and acts as a survival signal in mature Ocs. RANKL also has a decoy receptor: OPG. When bound to OPG, RANKL is blocked and cannot bind to RANK. Experimental work performed in mice has shown that the increase in Mks leads to a high bone mass phenotype[17-23]. *In vitro* studies have shown that Mks have the capacity to negatively regulate Oc recruitment and activity[24] and that this effect would be associated with a different factor, other than OPG[24,25], which has not been identified to date. *In vivo*, however, the increase in medullary Mks was observed together with an increase in the number of Ocs[19,23].

Considering the functional unit formed by bone and BM, it was observed that, in addition to their well known effect on bone tissue, some BPs cause marked alterations in hemopoiesis at the level of several progenies[25-28] including differentiation of lymphocytic cells to an interferon producing phenotype[29,30], thus also rendering them useful in hematology and oncology.

Monosodic Olpadronate (OPD, dimethyl pamidronate, Gador SA) is a N-BP. It is similar to alendronate in potency and gastric tolerance to the drug[31]. It has been used successfully in humans to treat Paget's disease, causing a significant decrease in serum bone formation and resorption markers[32]. Experimental studies have shown it to effectively prevent bone loss associated with supraphysiologic doses of thyroxin[33], renal osteodystrophy[34], and local bone loss associated with experimental periodontitis[35]. It was even found to improve the mechanical properties of long bones in healthy animals[36]. Although a number of works on the antirresorptive effect of OPD have been reported, there are no studies on the effect of OPD on Oc morphology and Mks.

The aim of the present work was to evaluate the effect of OPD on osteoclasts, and megakaryocytes using histochemical, immunohistochemical and histomorhometric studies in an *in vivo* experimental model.

Materials and methods

Experimental animals

Sixty two female Wistar rats aged 60 days and weighing 160±10 gr were divided into two groups. Housing conditions included galvanized wire cages, five animals per cage, 21-24 ºC temperature, 52-56% humidity and 12-12 hs light-dark cycles. The animals had free access to water and food (standard rat-mouse diet, Cooperación, Argentina) containing 23% protein, 1-1.4% Calcium and 0.5-0.8% phosphorous[37]. Experimental animals were injected intraperitoneally with OPD in a dose of 0.3 mg/kg of body weight (Gador SA, Argentina) once a week during five weeks. The Sham group received saline solution following the same protocol. Body weight was recorded weekly to adjust the dose to body weight. One week after the last dose (OPD or vehicle) the animals were anesthetized and blood samples were obtained by cardiac puncture, after which all the animals were sacrificed.

The Guide for the Care and Use of Laboratory Animals (NRC 1996) was observed.

Biochemical determinations

Serum calcium, bone isoenzyme alkaline phosphatase (bAP, kinetic method using precipitation with wheat-germ lectin) and osteocalcin (OC) (by EQLIA method) were measured.

Hemograms including leukocyte formula and platelet counts (hemocytometry using laser and/or impedance analyzers) were performed.

Histology, histochemistry and immunohistochemistry

After sacrifice, the femurs, tibiae, spleen, kidneys and liver were extracted from each animal.

Right tibiae and spleen were dissected and weighed using a precision scale. The lateral and anteroposterior width of the diaphysis and the total length of the tibia were measured using a Vernier caliper. Prior to fixing, the distal epiphysis of each tibia was sectioned longitudinally and gently imprinted on a slide to obtain Ocs ("epiphyseal bone imprints").

The extracted material and the "epiphyseal bone imprints" were fixed in 4% formaldehyde buffered solution at room temperature or 4˚C, according to the corresponding protocol. The mineralized material was decalcified in 10% EDTA at 4˚C for 30 days, dehydrated in graded alcohols and embedded in paraffin.

Seven micron-thick longitudinal sections of the tibiae and femurs were obtained.

Hematoxylin and eosin staining

The spleen, liver, kidney, left tibia samples were processed for routine hematoxylin-eosin staining in order to perform histological and histomorphometric studies.

Tartrate Resistant Acid Phosphatase (TRAP) Histochemistry

Histochemical Tartrate Resistant Acid Phosphatase (TRAP)[38] detection was performed in left tibia samples and "epiphyseal bone imprints".

Immunohistochemical detection of RANKL

Immunohistochemical detection of receptor activator of NFκB ligand (RANKL) was performed in right femur and spleen samples.

Sections were deparaffinised in xylene and washed in graded alcohols (1˚ethanol, 2˚methanol). The activity of endogenous peroxidase was inhibited during 30 min using a 3% H_2O_2 solution in 100% methanol. The slides were immersed in 0.1% Tween /Phosphate Buffered Saline (PBS) solution for 30 minutes to unmask the antigenicity of the tissue, and then rinsed with PBS. Primary goat polyclonal antibody to RANKL (Santa Cruz Biotechnology, Santa Cruz, CA. N-19: sc-7628)

was used at a concentration of 1:150 in a solution 1% albumin in PBS. The tissue was incubated with the primary antibody overnight at 4°C. For control experiments, sections were incubated with non-immune rabbit IgG in place of the primary antibody. After washing in PBS, the avidin-biotin-peroxidase complex (ABC) technique was performed: biotinylated rabbit anti-goat IgG and peroxidase-conjugated streptavidin. For visualization of reaction products, the sections were immersed in 0.02% 3.30-diaminobenzidine (DAB) in 0.01M PBS solution (pH 7.4) at room temperature for 7 to 10 min. The sections were then counterstained with hematoxylin.

Immunohistochemical detection of TUNEL

Immunohistochemical detection of terminal deoxynucleotidyl transferase- mediated dUTP-biotin nick end labelling (TUNEL)[39] (Apop Tag plus Peroxidase *in Situ* Apoptosis Detection Kit, Chemicon International, Canada) was performed in right femur samples. Briefly, sections were deparaffinised in xylene (3 washes of 5 min), rehydrated in graded alcohol solutions and washed in PBS for 5 min. For protein digestion Proteinase K (20 μg/mL) was used for 15 min, washed in two changes of dH_2O for 2 min and blocking of endogenous peroxidase was in 3% hydrogen peroxide in PBS. Following, the sections were rinsed in PBS, and incubated in a humidifier chamber with TdT enzyme at RT for 1 hour. After washing buffer, anti digoxigenin conjugate was applied; and sections were incubated for 30 min at RT, washed in PBS and treated with peroxidase substrate (3.30-diaminobenzidine: DAB) was used for 3 to 6 min. Sections were then counterstained with hematoxylin.

Histomorphometric measurements

Determinations of proximal tibia and distal femur bone tissue sections were performed in the middle third of subchondral trabeculae using Image Pro Plus 4.5 software. This area (2 mm^2) contains subchondral trabeculae corresponding to primary and secondary spongiosa.

Static histomorphometric studies were performed using parameters described by Parfitt[40] and other parameters defined in this work.

Hematoxylin-eosin stained spleen sections:

- Percentage of total area corresponding to red pulp (% red pulp).
- Megakaryocyte number (N.Mk/mm^2): number of Mk per area unit mm^2 (red pulp).

Hematoxylin-eosin stained tibia sections:

- Bone volume (% BV/TV) (%): the percentage of cancellous bone within the total measured area.
- Osteoclast number (N.Oc/mm^2): the number of Ocs in the measured area.
- Number of nuclei per osteoclast (N.nucl/Oc): the mean value was calculated.

Tibia sections processed for TRAP detection

- Number of TRAP+ osteoclasts (N.TRAP+Oc/mm^2).
- Percentage of TRAP+osteoclasts (% TRAP+Oc).
- Osteoclast Cell Volume (Oc CV) (μm^2): determined on "epiphyseal bone imprints" presenting complete cells.

Femur sections processed for TUNEL labeling:

- *Percentage of TUNEL positive osteoclasts (% TUNEL+Oc)*. Results were then typed according to the presence of TUNEL+Ocs with and without apoptotic morphology. Therefore, four categories were established to type Ocs according to their features: A. Apoptotic morphology TUNEL+; B. Apoptotic morphology TUNEL -; C. Non-apoptotic morphology TUNEL +; and D. Non-apoptotic morphology TUNEL-. After measuring femur TUNEL sections, double staining with TRAP was performed to confirm osteoclastic cell lineage.

Femur sections processed for immunohistochemical detection of RANKL:

- Percentage of total bone surface found to be RANKL positive (% RANKL+S/BS).
- Number of RANKL+osteoclasts (N. RANKL+Oc) (/mm^2).
- Percentage of RANKL+osteoclasts (% RANKL+Oc).
- Megakaryocyte number (N.Mk/mm^2).
- Number of RANKL+megakaryocytes (N. RANKL+Mk) (/mm^2).
- Percentage of RANKL+megakaryocytes (% RANKL+Mk).
- Presence of apoptotic morphology in osteoclasts.

Statistical Studies

The results are expressed as mean ± standard deviation. Student's t test, Mann Whitney's Rank Sum Test, or Mc Nemar's test were used according to the type and distribution of data. Data were analyzed using Primer (Mc Graw-Hill 1992) software. Values of p below 0.05 were considered statistically significant.

Results

Body weight

No significant differences were observed between groups throughout the experiment (Figure 1).

Biochemical Determinations

Significantly lower calcemia and osteocalcin values were observed in the experimental group (calcemia: Sham 4.9±0.1 vs OPD 4.6±0.07 mEq/l, $p<0.05$, osteocalcin: Sham 18.4±2.9 vs OPD 12.4±0.007 ng/ml, $p<0.05$) whereas no differences in bAP were found (97±1.4 vs OPD 102±11.3 IU/l, $p>0.05$).

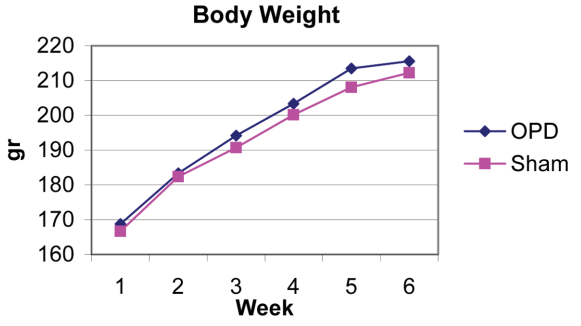

Figure 1. No differences in body weight were observed between groups (p>0.05).

Hemogram with platelet counts: No differences were observed between groups when comparing the studied parameters. It is noteworthy that a non-significant decrease in the number of platelets per mm^3 was observed in the OPD treated group compared with the Sham group (Sham $6.87x10^5 \pm 0.83x10^5$ vs OPD $7.32x10^5 \pm 0.76x10^5$, p=0.3).

Right tibia and spleen weight: OPD treated animals exhibited higher tibia weight values: 560±30 mg vs 510±30 mg in the sham group (p<0.001). No differences in bone length or width were observed. Experimental animals showed higher spleen weight values than the Sham group: 530±40mg vs. 490±54 mg (p<0.05).

Histologic evaluation of liver and kidney: H&E stained liver and kidney sections were evaluated qualitatively under a light microscope. No structural alterations were detected.

Histomorphometry

- Spleen.

The percentage of the total area corresponding to red pulp remained unchanged: Sham 32.4±9.5%, OPD 36.4±10%, p>0.05. A significant increase in the number of Mks per mm^2 of red pulp was observed: Sham group: 0.33±0.08 and OPD group: 0.87±0.3 (p<0.05). No RANKL positive Mks were detected in any of the spleen samples (Figure 2).

- Tibia and femur:

The studied histomorphometric parameters are shown in Table 1.

Femur bone volume was significantly higher in the OPD treated group although inhibition of bone resorption was observed; the treated group exhibited a higher number of Ocs (Figure 3), which were larger, presented a larger number of nuclei, and greater loss of polarity (Figure 4). TRAP expression was similar in both groups. The technique evidenced the lower degree of vacuolization in the experimental group and the presence of a more homogenous cytoplasm.

Similarly to Ocs, the total number of Mk/mm^2 (both RANKL positive and negative) was higher in the OPD treated group (Figure 5). The percentage of RANKL+Mks and Ocs was similar in both groups. However, due to the larger number of total Mks, the number of RANKL+Mks per area unit was significantly higher in the OPD treated group (Table 1, Mk: Figure 5). Values corresponding to mandibular interradicular bone (data not shown) were similar to those of tibiae and femurs.

	Sham	OPD
Tibia		
BV/TV (%)	14.3±6#	26.5±8.1#
Osteoclast histomorphometry		
Tibia		
N. Oc/TA (/mm^2)	47.7±11.1#	72.4±20.6#
N.nucl/Oc	4±0.6#	6.5±1.2#
N.OcTRAP+(/mm^2)	40.1±18.3	63.2±32.2
Oc TRAP+(%)	76.6±26	71±19
CV Oc (μm^2)	729±439#	1643±1228#
Femur		
N.OcTUNEL+(/mm^2)	0.15±0.31*	4±2.5*
Oc TUNEL+(%)	0.55±1.1*	7.7±4.3*
N.Oc RANKL+(/mm^2)	4.8±3.2	7.4±5.5
Oc RANKL+(%)	19±11.2	15.1±9
Megakaryocyte histomorphometry		
Femur		
N. MK (/mm^2)	29.9±5.6#	42.4±7#
N. MK RANKL+(/mm^2)	26.5±3.9#	37.5±6.1#
MK RANKL+(%)	87.8±11	92.4±9.9

Table 1. Histomorphometric parameters in tibia and femur. *:p<0.05, #: p<0.001.

TUNEL and RANKL Immunohistochemistry

Relation between immunolabeling and apoptotic morphology in Ocs.

It must be pointed out that although TUNEL+Ocs were found in the Sham group, they did not present apoptotic morphology. However, Ocs observed in the OPD treated group presented morphological features compatible with different apoptotic stages (Figure 6). All the morphological characteristics of apoptotic cells[41], such as round shape, chromatin condensation and margination, nuclear and cytoplasmic fragmentation, blebbing, and finally, the formation of apoptotic bodies were observed. TRAP labeling was used in order to confirm osteoclastic lineage (Figure 6). The relation between apoptotic morphology and positive TUNEL expression was studied in femur samples. Features corresponding to the four categories that were established are shown in Figure 7. In order to compare the Sham and experimental groups as regards the number of cells in each category, the results were expressed as a percentage (Table 2).

The same categories were applied to study Ocs and RANKL expression. The results are expressed as a percent-

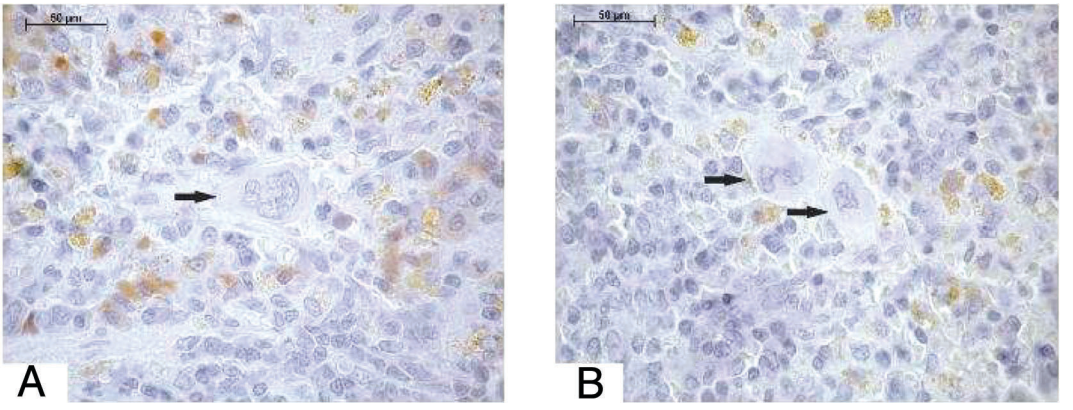

Figure 2. Splenic Mk (arrows) were all negative for RANKL detection in both groups: A. sham, B. OPD. Original magnification 1000X.

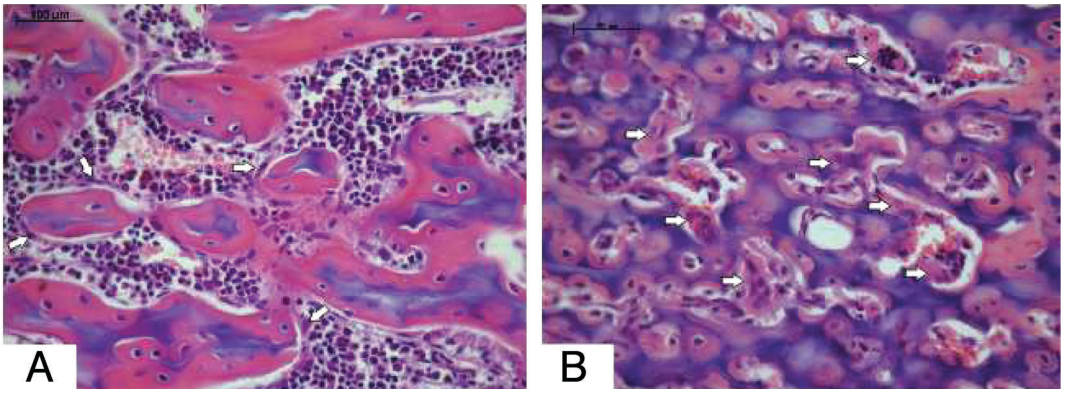

Figure 3. OPD increased the number of Ocs (arrows) by unit area. A. Sham, B. OPD. Femur, H-E staining. Original magnification 400X.

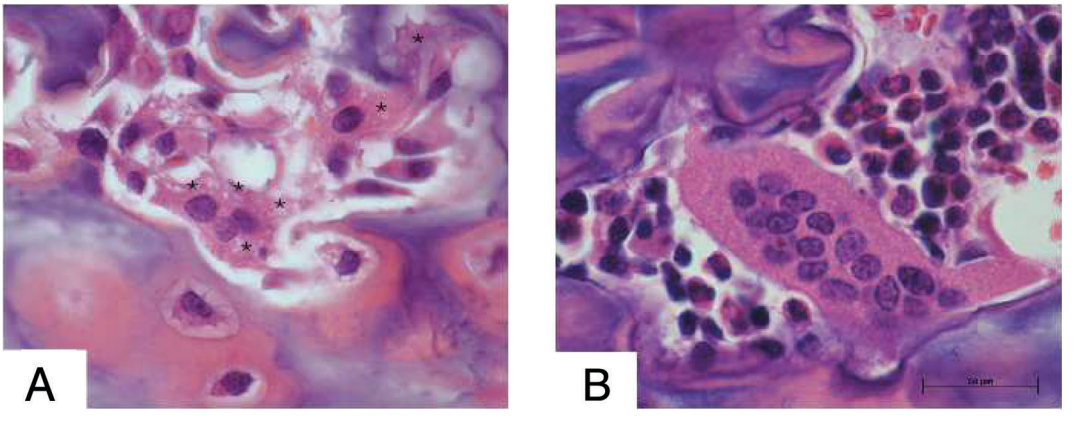

Figure 4. Sham Ocs were smaller, more vacuolated (*), attached to the bone surface, and had fewer nuclei. OPD Ocs were larger, less or not vacuolated, had more nuclei, and showed no cell polarity. H&E. Femur, H-E staining. Original magnification 1000X, bar represents 50 μm.

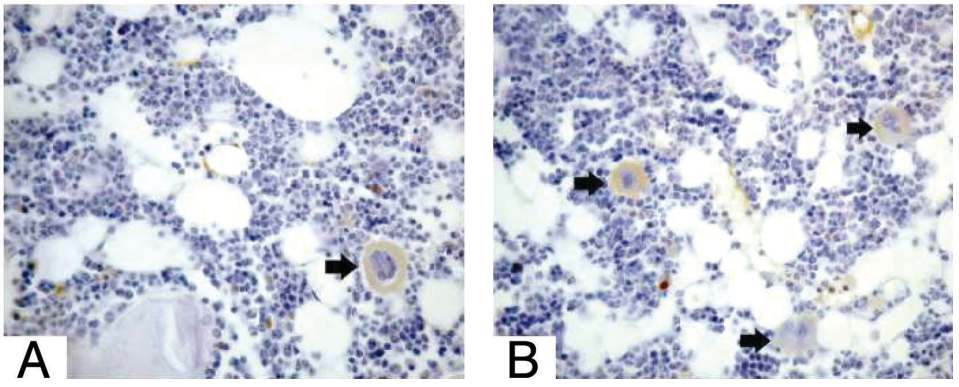

Figure 5. Immunohistochemical detection of RANKL in Mk (Mk RANKL+/mm^2): Sham group: 25.6±16; OPD group: 46±15.2 ($p<0.05$). Femur. Original magnification 400X.

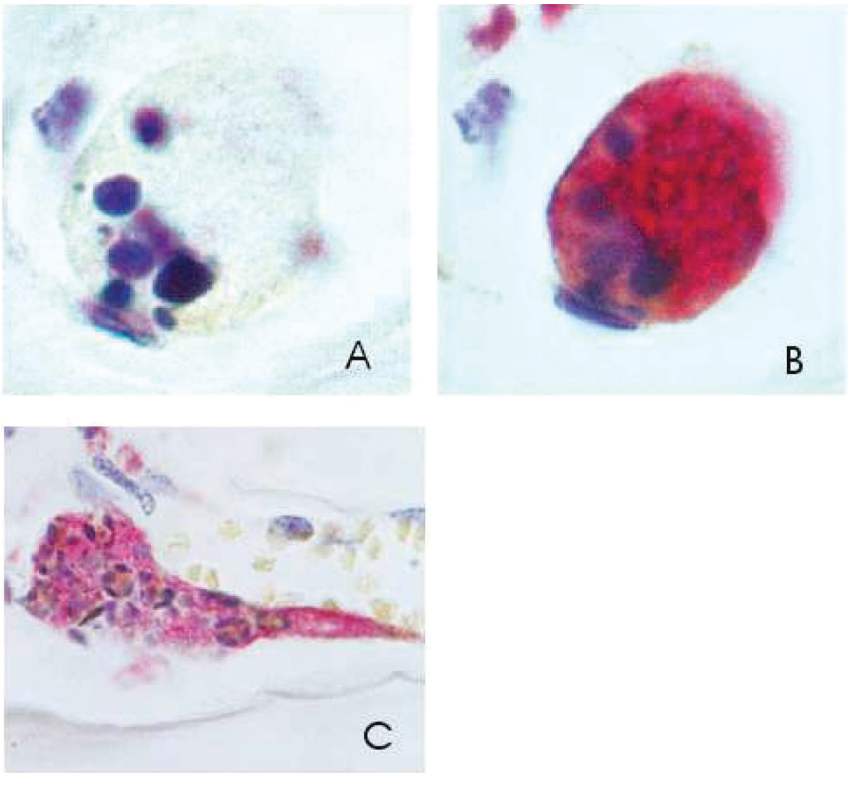

Figure 6. Double staining (TUNEL and TRAP) was performed to confirm osteoclastic cell lineage. A- TUNEL, B- and C-TUNEL plus TRAP, A- and B- show a late stage of apoptosis with nuclear fragmentation, C- stage of apoptosis previous to nuclear fragmentation. Original magnification 1000X.

age and are shown in Table 3. Statistically significant association was found between apoptotic morphology and RANKL expression in Ocs.

Sixty percent of Ocs presenting apoptotic morphological features in the OPD group expressed RANKL. Although only 4 cells exhibiting morphological features compatible with apoptosis were found in the Sham group, 3 of these cells (75%) expressed RANKL. Our results showed statistically significant association between apoptotic morphology and RANKL expression ($p<0.001$, Mc Nemar's test, see Table 4 and Figure 8). Likewise, cells presenting non-apoptotic morphology were found to be RANKL- in both Sham and OPD animals. According to our results, cells presenting apoptotic morphology express RANKL, whereas those without apoptot-

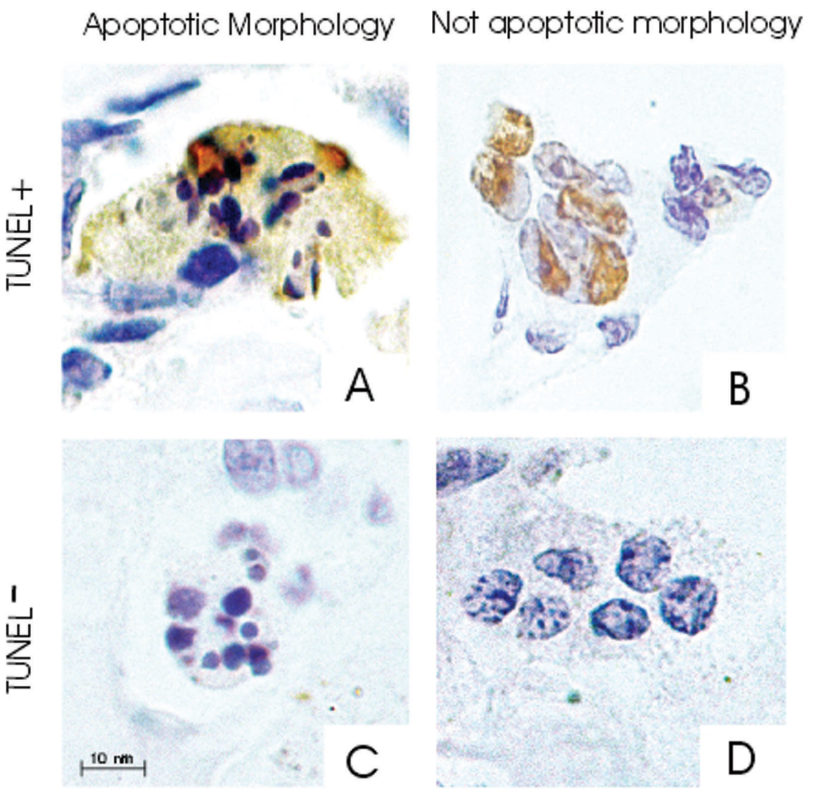

Figure 7. TUNEL detection. Ocs were classified into 4 categories according to the presence of apoptotic morphology and TUNEL detection. Each Oc was included in one of the following categories: A- Apoptotic morphology TUNEL+, B- Non apoptotic morphology TUNEL+, C-Apoptotic morphology TUNEL-, D- Non apoptotic morphology TUNEL-. Original magification 1000X.

	Apoptotic morphology		Non-apoptotic morphology	
	Sham	OPD	Sham	OPD
TUNEL+	0	4.5±4.1	0.55±1	3.25±2.3
TUNEL-	0	2.3±1.6	99.45±1*	90±6*
Total	0	6.8	100	93.2

Table 2. TUNEL detection in Ocs (femur). The results are expressed as mean±SD of the percentages (%).*p<0.05. The percentage of TUNEL+Ocs, irrespective of their morphology, was also higher in the OPD treated group. Number of studied Ocs: 467. (p<0.05, Table 1) (Mann Whitney's test).

	Apoptotic morphology		Non-apoptotic morphology	
	Sham	OPD	Sham	OPD
RANKL+	2.3±3.5	4.15±3.5	16.7±10.8	10.9±8.9
RANKL-	0	3±3.3	81±11.2	82±11.6
Total	2.3	7.15	97.7	92.9

Table 3. RANKL detection in Ocs (femur). Number of studied Ocs: 395. The results are expressed as mean±SD of the percentages (%); p>0.05, Mann Whitney's test.

ic morphology do not express RANKL (p<0.001) (Figure 9).

Active osteoblasts, which present abundant basophil cytoplasm, were RANKL- whereas lining cells were clearly RANKL+.

Discussion

The present study shows the effects of an amino-bisphosphonate (OPD) on anatomically or functionally related tissues, as is the case of bone and hemopoietic tissues (bone marrow and spleen).

BPs inhibit Oc mediated bone resorption; their effect on Ocs has been described extensively since 1975[42]. According to a number of authors, BPs lead to Oc apoptosis[1,8,9] alter the integrity of the cytoskeleton[5-7] and inhibit recruitment causing a diminution in the number of Ocs.

A number of studies have shown that BPs decreases Oc recruitment[43-45] whereas other works conclude that BPs affect the activity of mature Ocs, having little or no effect on recruitment[46]. However, our study shows a significant

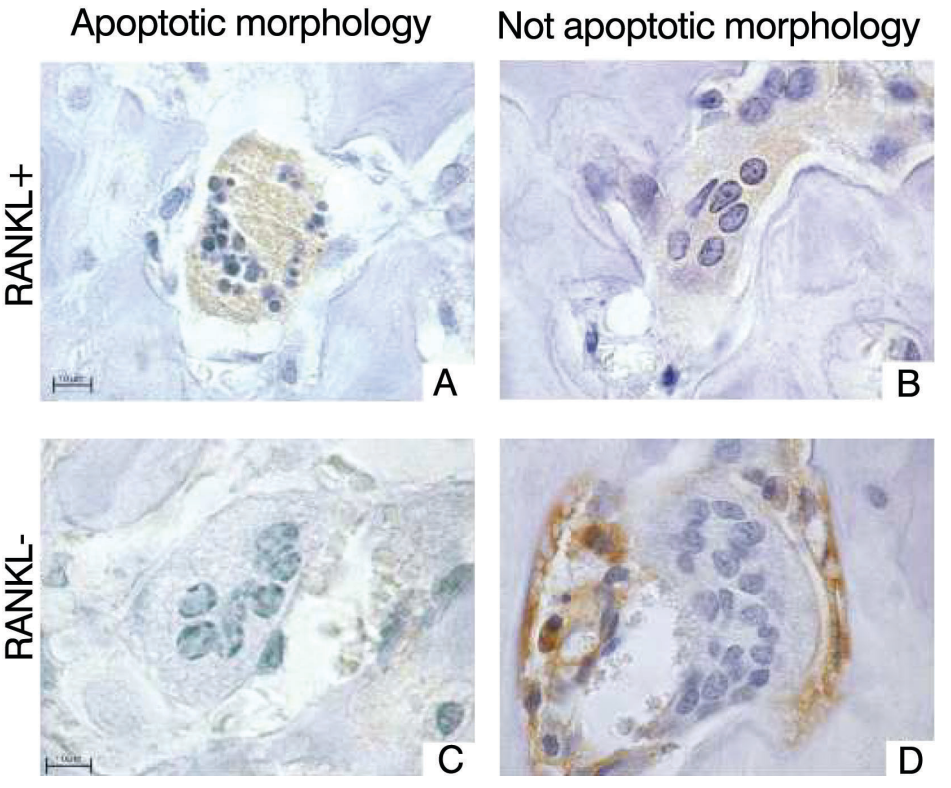

Figure 8. Immunohistochemical detection of RANKL Ocs were divided into 4 categories according to the presence of apoptotic morphology and RANKL detection. Ocs were classified as: A- Apoptotic morphology RANKL+, B- Non apoptotic morphology RANKL+, C- Apoptotic morphology RANKL-, D- Non apoptotic morphology RANKL-. The presence of apoptotic morphology was highly associated with RANKL expression (Mc Nemar's test, $p<0.001$). Original magnification 1000X, microphotographs correspond to OPD group.

increase in Oc number and size, more nuclei per cell, and a loss of polarity in the OPD group. TRAP detection was similar in both groups, in agreement with other studies reported in the literature[6]. The cytoplasm of Ocs corresponding to OPD treated animals showed less vacuolization possibly indicating less phagocytic activity. TRAP staining of bone imprints shows whole cells, and thus allows evaluating cell volume. The results obtained using TRAP staining were consistent with the histological findings, i.e. larger Ocs with a larger number of nuclei. Our observations are in keeping with a previous work carried out at our laboratory evaluating OPD in experimental periodontitis[35], and with reports by Miller et al[46], Marshall et al[47], Endo et al[48], Nakamura et al[25], Smith et al[49], and Weinstein et al[50] among others. In 1977 Miller et al[46], found ethane-1-hydroxy-1,1diphosphate (EHBP) treated animals to exhibit an increase in the number of Ocs and of their nuclei due to an increase in the differentiation of precursor cells to mature Ocs. The authors demonstrated the latter using tritiade timidine DNA labeling. Marshall et al[47] observed these same features in Ocs of experimental animals treated with an aminoBP (3-amino-1-hydroxypropylidene)-1,1-bisphosphonate (APD), and demonstrated the increase in precursor cell differentiation to mature Ocs using 5-bromo-2'-deoxyuridine (BrdU) nuclei labeling. In 2004, Smith et al[49] observed the same results in zoledronate treated animals. In an *in vivo* study using an aminoBP (AHBuBP), Endo et al[48] and Nakamura et al[25] observed similar findings to those reported here: loss of cell polarity, the ruffled border, and the clear zone in treated Ocs. The authors also found alterations in all monocytic lineage cells, and not only in Ocs. According to their results aminoBP caused marked depletion of medullary macrophages disorganizing erythroblastic islands, turning the bone marrow whitish, and initiating compensatory erythropoiesis in the spleen resulting in splenomegaly. We also observed splenomegaly in OPD treated animals. Conversely, we did not find whitish bone marrow. In addition, we observed a significant increase in the number of bone marrow MKs in OPD treated animals. Alves-Rosa et al, 2003[26] used clodronate to induce bone marrow macrophage depletion and found an increase in megakaryocytopoiesis and thrombocytopoiesis. In a later study[51] the authors concluded that factors secreted by macrophages negatively regulate the Mk compartment. Based on the findings reported by Nakamura[25], Alves Rosa[26] and Landoni[51] and the results obtained in this study, it could be posited that the increase in

Sham	Apoptotic morphology	Non-apoptotic morphology	
RANKL+	3 (75%)	21 (17%)	
RANKL-	1 (25%)	102 (83%)	
Total	4 (100%)	123 (100%)	127
OPD	**Apoptotic morphology**	**Non-apoptotic morphology**	
RANKL+	9 (60%)	28 (11%)	
RANKL-	6 (40%)	225 (89%)	
Total	15 (100%)	253 (100%)	268

Table 4. RANKL detection and apoptotic morphology in Ocs (femur). The presence of apoptotic morphology was associated with RANKL expression. Number of studied Ocs: 395. 127 from Sham group and 268 from OPD group. ($p<0.001$, Mc Nemar's test).

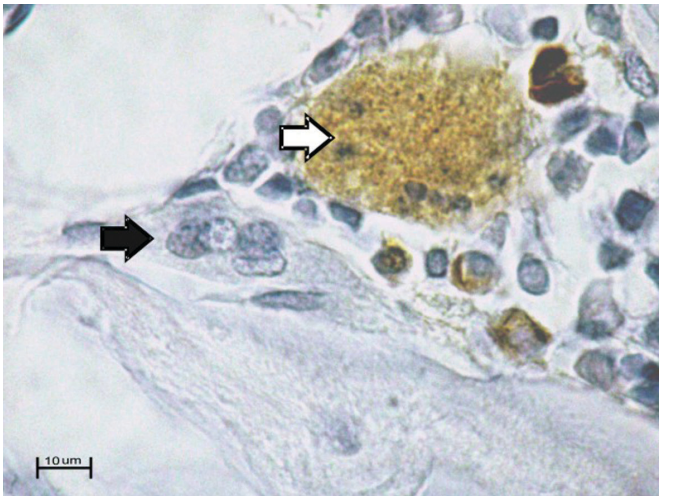

Figure 9. Immunohistochemical detection of RANKL in femur. Ocs without apoptotic morphology were RANKL - (black arrow) and Ocs with apoptotic morphology were RANKL + (white arrow). Original magnification 1000X, microphotograph corresponds to OPD group.

the number of Mks observed in the OPD-treated group is related with an alteration in differentiation pathways from monocytes macrophages/Ocs. OPD may therefore induce differentiation of monocytes to osteoclastic lineage cells by means of a mechanism which remains to be clarified.

Mks have been reported to express proteins (or the mRNA that codes them), such as osteocalcin[52], OPG[14] and RANKL[15,16], that were previously thought to be specific to bone cells and matrix. A number of *in vitro* studies have demonstrated the relation between bone cells and MKs: co-culture of Mks and osteoblasts (Obs) stimulates OPG expression in Obs and decreases RANKL expression[53], and co-culture of Ocs and Mks causes a decrease in the number of Ocs[21]. In addition, *in vivo* studies in GATA-1 or NF-E2 deficient mice, two transcriptional factors required for normal Mk development, revealed that accumulation of immature Mks in the BM is associated with high bone mass phenotype[19,20,23]. In a study in GATA-1^{low} mice with osteosclerotic phenotype, Garimella et al[23], 2007, found an increase in the number of Ocs despite the osteosclerotic condition. The authors suggest that osteosclerosis may be mediated by bone morphogenetic proteins (BMP's) secreted by Mks and Obs. The bone phenotype described in GATA-1^{low} mice is very similar to that observed in our group of OPD treated animals, which also exhibited an increase in bone volume and in the number of Ocs and Mks, and a decrease in circulating platelets; the latter, however, did not reach statistical significance. In the present study, the number of Ocs and Mks was significantly higher in the OPD-treated group. Given that RANKL signals Oc recruitment, the increase in RANKL+Mk, and therefore the increase in RANKL in the BM microenvironment, may explain the increase in Ocs reported in our study and in previous *in vivo* studies using different BPs[25,47-52]. In the present study, spleen Mks did not express RANKL, suggesting that expression of certain cytokines is not constitutive of Mks but depends on their microenvironment.

The data obtained in OPD treated animals show an increase in the number of Mks and in RANKL+Mk. In turn, the increase in the number of RANKL+Ocs suggests that the increase in Oc recruitment and size may be associated with an increase in RANKL synthetized by Mks and Ocs in the BM microenvironment. Our results show RANKL expression in Ocs, mainly in those undergoing apoptosis. Although the presence of RANKL mRNA in Ocs has been described[16], to our knowledge this is the first study to report RANKL expression in Ocs presenting morphological features compatible with apoptosis and statistically significant association between RANKL expression in Ocs and apoptotic morphology. It could be thought that when Ocs enter apoptosis, they synthetize RANKL thus inducing recruitment of new Ocs.

As regards evaluation of Oc apoptosis using TUNEL, an increase in TUNEL+Ocs was found in OPD treated animals (8% vs 0.5 % in controls). TUNEL was detected in Ocs with and without apoptotic morphology (see Figure 4). Moreover, only two percent of TUNEL-Ocs exhibited apoptotic morphology. These findings not only show that BPs increase Oc apoptosis[1,8,9,54], but also that TUNEL is not expressed in all the stages of the process. It is well documented that TUNEL is a nuclear marker of apoptosis, since it allows detecting apoptosis-induced DNA fragmentation. Regarding our finding of chromogen in Oc cytoplasm, it is in agreement with the findings of Ito et al who described that "some nuclei were disrupted, as evidenced by the rupture of the nuclear envelope, leading to the leakage of nuclear components in the citoplasm.

Although an increase in the number of apoptotic Ocs was

observed in this study, cell death was not sufficient to diminish the number of Ocs, demonstrating that the inhibitory effect of OPD on bone resorption is not associated with Oc apoptosis but with other mechanisms.

The results obtained in this study show that OPD no only exerts an effect on Ocs but also on Mks. The increase in Mks in BM and in the spleen suggests a direct effect of OPD on megakaryopoiesis. In addition, the increase in RANKL+ Mks and Ocs may be the cause of the increase in Oc recruitment observed in OPD treated animals.

Further studies on the effect of BPs on Mks should be conducted in order to elucidate the complex mechanism of action by which these drugs exert their effect on the bone-bone marrow functional unit, and thus gain a better understanding of the clinical and therapeutic implications of BP therapy.

Acknowledgements

The authors acknowledge the collaboration of animal laboratory technician Marianela Lewicki and histology laboratory technician Ana María Gómez, Department of Histology and Embryology, School of Dentistry, University of Buenos Aires.

The authors thank Prof. Dr. Ricardo Macchi (Department of Dental Materials, School of Dentistry, University of Buenos Aires) for his assistance in the statistical analyses, laboratory technician Víctor Tomasi (Department of Oral Pathology, School of Dentistry, University of Buenos Aires), the staff of the Biochemical Laboratory of CEMIC, (Buenos Aires, Argentina) for performing the biochemical determinations, Gador SA (Buenos Aires, Argentina) for supplying monosodium olpadronate and Nélida Mondelo from Gador SA for her support.

This investigation was supported in part by grants O 013 from the University of Buenos Aires, PIP 6010 from Consejo Nacional de Investigaciones Científicas y Tecnológicas (CONICET) and from Roemmers Foundation 2007-2009.

References

1. Hiroi-Furuya E, Kameda T, Hiura K, Mano H, Miyazawa K, Nakamaru Y, Watanabe-Mano M, Okuda N, Shimada J, Yamamoto Y, Hakeda Y, Kumegawa M. Etidronate (EHDP) inhibits osteoclastic-bone resorption, promotes apoptosis and disrupts actin rings in isolate-mature osteoclasts. Calcif Tissue Int 1999;64:219-23.
2. Van Beek E, Pieterman E, Cohen L, Löwik C, Papapoulos S. Farnesyl pyrophosphate synthase is the molecular target of nitrogen-containing bisphosphonates. Biochem Biophys Res Commun 1999;264:108-11.
3. Dunford JE, Thompson K, Coxon FP, Luckman SP, Hahn FM, Poulter CD, Ebetino FH, Rogers MJ. Structure-activity relationships for inhibition of farnesyl diphosphate syntase *in vitro* and inhibition of bone resorption *in vivo* by nitrogen-containing bisphosphonates. J Pharmacol Exp Ther 2001;296:235-42.
4. Van Beek ER, Löwik CWGM, Papapoulos SE. Bisphosphonates supress bone resorption by a direct effect on early osteoclast precursors without affecting the osteogenic capacity of osteogenic cells: the role of protein geranylgeranylation in the action of nitrogen-containing bisphosphonates on osteoclast precursors. Bone 2002;30:64-70.
5. Murakami H, Takahashi N, Sasaki T, Udagawa N, Tanaka S, Nakamura I, Zhang D, Barbier A, Suda T. A possible mechanism of the specific action of bisphosphonates on osteoclasts: tiludronate preferentially affects polarized osteoclasts having ruffled borders. Bone 1995;17:137-44.
6. Murakami H, Takahashi N, Tanaka S, Nakamura I, Udagawa N, Nakajo S, Nakaya N, Abe M, Yuda Y, Konno F, Barbier A, Suda T. Tiludronate inhibits protein tyrosine phosphatase activity in osteoclasts. Bone 1997;20:399-404.
7. Koshihara Y, Kodama S, Ishibashi H, Azuma Y, Ohta T. Reversibility of alendronate-induced contraction in human osteoclast-like cells formed from bone marrow cells in culture. J Bone Miner Metab 1999;17:98-107.
8. Ito M, Amizuka N, Nakajima T, Ozawa H. Ultrastructural and citochemical studies on cell death of osteoclasts induced by bisphosphonate treatment. Bone 1999;25:447-52.
9. Benford HL, Mc Gowan WA, Helfrich MH, Nuttall ME, Rogers MJ. Visualization of bisphosphonate-induced Caspase-3 activity in apoptotic osteoclasts *in vitro*. Bone 2001;28:465-73.
10. Halleen JM, Alatalo SL, Suominen H, Cheng S, Janckila AJ, Väänänen HK. Tartrate-resistant acid phosphatase 5b: a novel serum marker for bone resorption. J Bone Miner Res 2000;15:1337-45.
11. Garnero P, Delmas PD. Biochemical markers of bone turnover: clinical usefulness in osteoporosis. Ann Biol Clin 1999;57:137-48.
12. Compston JE. Bone and bone marrow: a functional unit. J Endocrinol 2002;173:387-93.
13. Yin T, Li H. The stem cell niches in bone. J Clin Invest 2006;116:1195-201.
14. Chagraoui H, Sabri S, Capron C, Villeval JL, Vainchenker W, Wedling F. Expression of osteoprotegerin mRNA and protein in murine megakaryocytes. Exp Hematol 2003;31:1081-88.
15. Bord S, Frith E, Ireland DC, Scott MA, Craig JI, Compston JE. Synthesis of osteoprotegerin and RANKL by megakaryocytes is modulated by oestrogen. Br J Haematol 2004;126:244-51.
16. Kartsogiannis V, Zhou H, Horwood NJ, Thomas RJ, Hards DK, Quinn JMW, Niforas P, Ng KW, Martin TJ, Guillespie MT. Localization of RANKL (receptor activator of NFκB ligand) mRNA and protein in skeletal and extraskeletal tissues. Bone 1999;25:525-34.
17. Wakikawa T, Shioi A, Hino M, Inaba M, Nishizawa Y, Tatsumi N, Morii H, Otani S. Thrombopoietin inhibits *in vitro* osteoclastogenesis from murine bone marrow cells. Endocrinology 1997;138:4160-66.
18. Villebal JL, Cohen Solal K, Tulliez M, Giraudier S, Guichard J, Burstein SA, Cramer EM, Vainchenker W,

Wendling F. High thrombopoietin production by hematopoietic cells induces a fatal myeloproliferative syndrome in mice. Blood 1997;90:4369-83.
19. Kacena MA, Gundberg CM, Nelson T, Horowitz MC. Loss of the transcription factor p45 NF-E2 results in a developmental arrest of megakaryocyte differentiation and the onset of a high bone mass phenotype. Bone 2005;36:215-23.
20. Kacena MA, Shivdasani RA, Wilson K, Xi Y, Troiano N, Nazarian A, Gundberg CM, Bouxsein ML, Lorenzo JA, Horowitz MC. Megakaryocyte-osteoblast interaction revealed in mice deficient in transcription factors GATA-1 and NF-E2. J Bone Miner Res 2004;19:652-60.
21. Kacena MA, Nelson T, Clough ME, Lee SK, Lorenzo JA, Gundberg CM, Horowitz MC. Megakaryocyte-mediated inhibition of osteoclast development. Bone 2006;39:991-99.
22. Kacena MA, Gundberg CM, Horowitz MC. A reciprocal regulatory interaction between megakaryocytes, bone cells, and hematopoietic stem cells. Bone 2006;39:978-84.
23. Garimella R, Kacena MA, Tague SE, Wang J, Horowitz MC. Expresión of bone morphogenetic proteins and their receptors in the bone marrow megakaryocytes of GATA-1^{low} mice: a posible rol in osteosclerosis. J Histochem Cytochem 2007;55:745-52.
24. Beeton CA, Bord S, Ireland D, Compston JE. Osteoclast formation and bone resorption are inhibited by megakaryocytes. Bone 2006;39:985-90.
25. Nakamura M, Yagi H, Endo Y, Kosugi H, Ishi T, Itoh T. A time kinetic study of the effect of aminobisphosphonate on murine haemopoiesis. Br J Haematol 1999;107:779-90.
26. Alves-Rosa F, Vermeulen M, Cabrera J, Stanganelli C, Capozzo A, Narbaitz M, Van Rooijen N, Palermo M, Isturiz MA. Macrophage depletion following liposomal-encapsulated clodronate (LIP-CLOD) injection enhaces megakaryocytopoietic and thrombopoietic activities in mice. Br J Haematol 2003;121:130-38.
27. Landoni VI, Vermeulen M, Van Rooijen N, Gomez S, Palermo S, Isturiz MA, Alves-Rosa F. Macrophage derive signalling regulates negatively the megakaryocyte compartment. Cell Mol Biol (Noisy le Grand) 2004; 50 Online Pub:OL667-75.
28. Giuliani AL, Graldi G, Veronesi M, Unis L, Previato A, Lorenzini F, Grandini G, Bergamini C, Vanara F, Wiener E, Wickramasinghe SN, Berti G. Aging of red blood cells and impaired erythropoiesis following prolonged administration of dichloromethylene diposphonate containing liposomes in rats. Eur J Haematol 2005;75:406-16.
29. Kunzman V, Bauer E, Wilhelm M. Gamma/delta T-cell stimulation by pamidronate. N Engl J Med 1999; 340:737-38.
30. Thompson K, Rogers M. Bisphosphonates and γδ T-cells: new insights into old drugs. BoneKEy-Osteovision 2006;3:5-13.
http://www.bonekey-ibms.org/cgi/content/full/ibmske
31. Roldan EJ, Perez Llore A, Ferretti JL. Olpadronate: a new amino-bisphosphonate for the treatment of medical osteopathies. Expert Opin Investig Drugs 1998;7:1521-38.
32. Mautalén C, Gonzalez D. Short-term therapy with oral olpadronate in very active Paget's disease. Bone 1999; 24:5(s)93S.
33. Zeni S, Gomez Acotto C, Di Gregorio S. Olpadronate prevents cortical and trabecular bone loss induced by supraphysiological dosis of thyroxine in ovariectomized rats. Medicina (B. Aires) 1998;58:453-5.
34. Tomat A, Gamba CA, Mandalunis PM, De Grandi MC, Somoza J, Friedman S, Zeni S. Changes in bone volume and bone resorption by olpadronate treatment in an experimental model of uremic bone disease. J Musculoskelet Neuronal Interact 2005;5:174-81.
35. Goya JA, Paez HA, Mandalunis PM. Effect of topical administration of monosodium olpadronate on experimental periodontitis in rats. J Periodontol 2006;77:1-6.
36. Ferretti JL, Mondelo N, Capozza RF, Cointry GR, Zanchetta JR, Montuori E. Effects of large dosis of olpadronate (dimethyl pamidronate) on mineral density, cross-sectional architecture and mechanical properties of rat femurs. Bone 1995;16(Suppl.):285S-293S.
37. Bernhart FW, Tomarelli RM. A salt mixture supplying the National Research Council estimates of the mineral requirements of the rat. J Nutr 1966;89:495-500.
38. Minkin C. Bone Acid Phosphatase: tartrate-resistant acid phosphatase as a marker of osteoclast Function. Calcif Tissue Int 1982;34:285-90.
39. Gavrieli Y, Sherman Y, Ben Sasson SA. Identification of programmed cell death *in situ* via specific binding of nuclear DNA fragmentation. J Cell Biol 1992;119:493-501.
40. Parfitt AM, Glorieux FH, Kanis JA, Malluche H, Meunier PJ, Ott SM, Recker RR. Bone histomorphometry nomenclature, symbols and units: report of the ASBMR Histomorphometry Nomenclature Comitee. J Bone Min Res 1987;2:595-610.
41. Kerr JF, Wyllie AH, Currie AR. Apoptosis: a basic biological phenomenon with wide-ranging implications in tissue kinetics. Br J Cancer 1972;26:239-57.
42. Miller SC, Jee WS. Ethane-1-hydroxy-1, 1-diphosphonate (EHDP) effects on growth and modeling of the rat tibia. Calciff Tissue Res 1975;18:215-31.
43. Sudhoff H, Jung JY, Ebmeyer J, Faddis BT, Hildman H, Chole RA. Zoledronic acid inhibits osteoclastogénesis *in vitro* and in a mouse model of inflammatory osteolysis. Ann Otol Rhinol Laryngol 2003;112:780-86.
44. Keles A, Grunes B, Difuria C, Gagari E, Srinivasan V, Darendeliler MA, Muller R, Kent R Jr, Stashenko P. Inhibition of tooth movement by osteoprotegerin vs. pamidronate under conditions of constant orthodontic force. Eur J Oral Sci 2007;115:131-36.
45. Breuil V, Cosman F, Stein L, Horbert W, Nieves J, Shen V, Lindsay R, Dempster DW. Human osteoclast formation and activity *in vitro*: effects of alendronate. J Bone Miner Res 1998;13:1721-29.
46. Miller SC, Jee WS, Kimmel DB, Woodbury L. Ethane-

1-hydroxy-1, 1-diphosphonate (EHDP) effects on incorporation and accumulation of osteoclast nuclei. Calcif Tissue Res 1977;22:243-52.
47. Marshall MJ, Holt I, Davie MWJ. Osteoclast recruitment in mice is stimulated by (3-amino1-hydroxypropylidene)-1,1bisphosphonate. Calcif Tissue Int 1993;8:45-50.
48. Endo Y, Nakamura M, Kikuchi T, Shinoda H, Takeda Y, Nitta Y, Kumagai K. Aminoalkylbisphosphonates, potent inhibitors of bone resorption, induce a prolonged stimulation of histamine synthesis and increase macrophages, granulocytes, and osteoclasts *in vivo*. Calcif Tissue Int 1993;52:248-54.
49. Smith EJ, Mc Evoy A, Little DG, Baldock PA, Eisman JA, Gardiner EM. Transient retention of endochondral cartilaginous matrix with bisphosphonates treatment in a long-term rabbit model of distraction osteogénesis. J Bone Miner Res 2004;19:1698-705.
50. Weinstein RS, Roberson PK, Manolagas SC. Giant osteoclast formation and long-term oral bisphosphonate therapy. N Engl J Med 2009;1:360:53-62.
51. Landoni VI, Vermeulen M, Van Rooijen N, Gomez S, Palermo M, Isturiz MA, Alves-Rosa F. Macrophage derived signaling regulates negatively the megakaryocyte compartment. Cell Mol Biol (Noisy-le-grand) 2004; 50 Online Pub:OL667-75.
52. Thiede MA, Smock SL, Petersen DN, Grasser WA, Thompson DD, Nishimoto SK. Presence of messenger ribonucleic acid encoding osteocalcin, a marker of bone turnover, in bone marrow megakaryocytes and peripheral blood platelets. Endocrinology 1994;135:929-37.
53. Bord S, Frith E, Ireland DC, Scott MA, Craig JIO, Compston JE. Megakaryocytes modulate osteoblast synthesis of type-1 collagen, osteoprotegerin, and RANKL. Bone 2005;36:812-18.
54. Hughes DE, Wright KR, Uy HL, Sasaki A, Yoneda T, Roodman GD, Mundy GR, Boyce BF. Bisphosphonates promote apoptosis in murine osteoclast *in vitro* and *in vivo*. J Bone Miner Res 1995;10:1478-87.